ASIA-PACIFIC JOURNAL OF CHEMICAL ENGINEERING
Asia-Pac. J. Chem. Eng. (2011)
Published online in Wiley Online Library
(wileyonlinelibrary.com) DOI:10.1002/apj.574

Research Article

Correlation of solubility of single gases/hydrocarbons in polyethylene using PC-SAFT

*Sunil K. Maity**

Department of Chemical Engineering, Indian Institute of Technology Hyderabad, Ordnance Factory Estate, Yeddumailaram 502205, Andhra Pradesh, India

Received 1 October 2010; Revised 31 January 2011; Accepted 13 February 2011

ABSTRACT: The knowledge of solubility of gases and hydrocarbons in polymer has enormous importance in the design and development of reactor, polymer foaming, and membrane separation processes. In this work, the solubility of gases and hydrocarbons in polyethylene was correlated using a thermodynamic model based on perturbed-chain statistical associating fluid theory (PC-SAFT). The experimental solubility data of various gases such as ethylene, carbon dioxide, nitrogen, methane, and hydrocarbons of up to chain length of seven in both molten and semicrystalline polyethylene has been reviewed and the suitability of the developed model based on PC-SAFT was then tested using the available solubility data in literatures for various gases and hydrocarbons. Furthermore, the optimum values of adjustable solvents-solute binary interaction parameters (Kij) of PC-SAFT at different temperatures have been estimated by regression of the PC-SAFT model using experimental solubility isotherms. A suitable correlation of Kij with temperature was then developed using the estimated Kij at different temperatures. The solubility calculated from the developed model using the estimated Kij was then compared to the experimental results and a reasonably good correlation was observed.

KEYWORDS: modeling; solubility; polyethylene; PC-SAFT; gases; hydrocarbons

INTRODUCTION

Polymer foaming processes are commonly used to produce foamed products of varying densities for applications that require attributes such as weight reduction, insulation, buoyancy, energy dissipation, convenience, and comfort.[1] The gaseous phase in any polymer foaming process is commonly derived using blowing agents. Two types of blowing agents are generally used in the polymer foaming process: chemical and physical blowing agents. Chemical blowing agents are chemical compounds which evolve gases under foam processing conditions through thermal degradation or chemical reactions. Physical blowing agents, on the other hand, are inert gases such as nitrogen and carbon dioxide; volatile hydrocarbons such as propane, butane, pentane, etc.; and low boiling point chlorofluorocarbons (CFCs), hydrofluorocarbons (HFCs) and hydrochlorofluoro-carbons (HCFCs). Owing to the environmental hazard posed by CFCs, HFCs, and HCFCs, there has been an increasing drive to replace these blowing agents with an environment friendly substitute. The solubility that determines the amount of blowing agent that can be absorbed by the polymer at a given temperature and pressure is a key issue to be considered in order to find an effective replacement of conventional blowing agents.

The knowledge of solubility of gases, especially monomers and solvents in polymers, is of considerable industrial importance for understanding and optimal design of final-treatment processes used for the production, degassing, and subsequent processing. For example, in the production of polyethylene, the polymerization product from the reactor contains a significant amount of an unreacted monomer, ethylene, which needs to be separated from polyethylene before being sent for further processing. Rational design of such separators requires knowledge of the equilibrium solubility of ethylene in liquid polyethylene at separator conditions. In the manufacture of polyvinyl chloride, the unreacted monomer, vinyl chloride, which exists in the polymerization products are harmful to the environment. The design of the devolatilization process used to remove those monomers needs knowledge of gas solubility in polymers at various temperatures and pressures.

During the gas-phase production of polyethylene, semicrystalline polyethylene is produced surrounding

**Correspondence to*: Sunil K. Maity, Department of Chemical Engineering, Indian Institute of Technology Hyderabad, Ordnance Factory Estate, Yeddumailaram 502205, Andhra Pradesh, India.
E-mail: sunil_maity@iith.ac.in; drsunilmaity@gmail.com

the catalytic sites.[2] Therefore, the gaseous monomers and co-monomers must be absorbed into and diffused through the amorphous polymer to reach the catalytic sites to continue further polymerization reactions. Thus, the rate of the polymerization reaction and the design of devolatilization equipments greatly depend on the solubility of gases in semicrystalline polymer.[3] Furthermore, the sorption of gases in semicrystalline polymers is important in numerous other applications, particularly where gas permeability plays an important role such as membrane separation processes. As the permeability coefficient is the product of the solubility and the diffusion constant, gas sorption is crucial in applications such as gas separation membranes and diffusion barrier materials.[4,5]

The experimental solubility data for various gases in polyethylene is very scarce in literature. The absence of suitable thermodynamic models for the polymer system properties and phase behavior makes the design of such kind of processes a tedious and time consuming one. Therefore, the availability of a validated thermodynamic model is quite desirable and essential for the design and development of such kind of processes, especially when the experimental data are rare. In the past, the modeling of fluid-phase equilibrium for polymer systems was usually done either based on activity coefficient models (Flory-Huggins, NRTL, UNIFAC) or the equation of state-based models (Sanchez-Lacombe, polymer-SRK).[6–8] Recently, Chapman *et al*.[9] derived the statistical associating fluid theory (SAFT) equation of state based on Wertheim's first-order thermodynamic perturbation theory for chain molecules. Numerous modifications and improvements of different versions of SAFT have been proposed and applied to various mixtures over the last 20 years, such as SAFT hard-sphere,[10,11] simplified SAFT,[12] SAFT Lennard–Jones,[13,14] perturbed-chain SAFT (PC-SAFT),[15] SAFT variable range (SAFT-VR),[16] and simplified PC-SAFT[17] to mention only a few. Among the several versions of SAFT, the PC-SAFT equation of state gained significant attention from both industry and academia because of its versatile applications. The PC-SAFT equation of state was developed based on the perturbation theory for chain molecules considering the pair potential of the segments of a chain by a modified square-well potential and it requires three pure-component parameters namely segment number (m), interaction energy (ε/k in K), and segment diameter (σ in °A). Moreover, the equation of state has one adjustable solvent–solute binary interaction parameter (Kij).

For correlation and prediction of fluid-phase equilibrium, the PC-SAFT has been applied extensively to the varieties of systems including polymers.[18,19] However, specific interactions, such as hydrogen bonding or a multipole interaction, was not considered in the original PC-SAFT. The equation of state was further extended to associating fluids,[20] copolymers,[21] and polar systems.[22] In recent years, several researchers used PC-SAFT to model liquid–liquid equilibrium of homo- and co-polymer systems,[23,24] gas solubility in molten polymer,[25,26] solid–liquid equilibrium polymer-solvents,[27] and high pressure co-polymer phase equilibrium.[28,29] On the other hand, the use of the SAFT type equation of state for modeling and correlation gas solubility in semicrystalline polymer was only limited to simplified SAFT[30,31] and SAFT-VR.[30,32] The PC-SAFT also finds a multitude of applications for calculation of critical points,[33–35] viscosity,[36] and surface tension[37] for multicomponent mixtures, and kinetic modeling of equilibrium-limited reactions,[38,39] and global-phase diagram.[40]

However, the correlation of gas solubility using PC-SAFT in molten and semicrystalline polyethylene is very scarce in open literature. Considering the enormous importance of the system, this work was undertaken to develop a thermodynamic model based on the PC-SAFT equation of state to correlate solubility gases and hydrocarbons in both molten and semicrystalline polyethylene. Moreover, in this article, a review of experimental solubility data for various gases such as ethylene, carbon dioxide, nitrogen, methane, and hydrocarbons of up to chain length of seven in both molten and semicrystalline polyethylene has been made to generalize the nature of solubility and the suitability of the developed model based on PC-SAFT was then tested using the available solubility data. Furthermore, in this work, the optimum values of Kij at different temperatures was estimated by regression of the PC-SAFT model using available experimental solubility isotherms and then a suitable correlation of Kij with temperature was developed for various gases and hydrocarbons–polyethylene (molten and semicrystalline polyethylene) systems.

MODELING OF SOLUBILITY OF GASES IN POLYMER

For any phase equilibrium, the fugacity (f) of any component in all the phases is equal under equilibrium conditions. For solubility of any component (i) of gas phase (G) in liquid polyethylene (L), one can write following equation.

$$f_i^G = f_i^L \tag{1}$$

By using the definition of fugacity, the above equation can be represented as follows:

$$\phi_i^G \; y_i^G \; P = \phi_i^L x_i^L \; P \tag{2}$$

The ϕ_i^G and ϕ_i^L represent the fugacity coefficient of component, i, in gas and liquid phase, respectively. As the molecular weight of the polymer is usually high,

DOI: 10.1002/apj

it is therefore reasonable to assume that the polymer remains entirely in the liquid phase. For solubility of a single gas, the mole fraction, y_i^G, become unity. The solubility of the single gas, x_i^L, in polyethylene can then be easily calculated using the following equation.

$$x_i^L = \frac{\phi_i^G}{\phi_i^L} \tag{3}$$

In this work, the fugacity coefficient of the various gases, ϕ_i^G, and molten polymer, ϕ_i^L, were calculated using the PC-SAFT equation of state developed by Gross and Sadowski.[15] The above equation is applicable for prediction of solubility of gases or vapors above the melting point of the polymer. The melting point of semicrystalline polyethylene is a function of crystallinity measured at 298 K and 1 atm as given by the following correlations for the polyethylene formed from two different catalysts, Ziegler-Natta (ZN) and metallocenes (Me).[32] The physical properties of polymer including the melting point, however, were not measured in most of the solubility studies reported in open literatures (Tables 2 and 3). Therefore, these equations are very useful to judge whether the polyethylene under experimental conditions is molten or semicrystalline.

$$T_m(\mathrm{ZN})(^\circ\mathrm{C}) = 13.689\omega_{\mathrm{crys},25}^2 + 5.015\omega_{\mathrm{crys},25} + 124.33 \tag{4}$$

$$T_m(\mathrm{Me})(^\circ\mathrm{C}) = -81.498\omega_{\mathrm{crys},25}^2 + 163.3\omega_{\mathrm{crys},25} + 63.415 \tag{5}$$

For completely crystalline polyethylene ($\omega = 1.0$), the calculated melting temperature based on these correlation is 416 and 418 K for ZN and Me catalysts, respectively. The melting temperature of semicrystalline polyethylene is lower than that of crystalline polyethylene as one can see from the above equations. For semicrystalline polyethylene below melting temperature, the amorphous fractions behave as a liquid-like structure despite being the solid phase and thus absorption of gases is limited to only the amorphous region and the crystalline region remains inaccessible to gas molecules.[3,41–43] When the gases are absorbed in the amorphous regions, a gas–liquid equilibrium theory for polymer solutions can be applied as governed by Eqn 3. As gas absorption is limited to the amorphous regions only, the solubility of gas per unit mass of amorphous polymer (S_{am}) is related to that of per unit mass of total polymer (S) as given by the following equation.

$$S_{\mathrm{am}} = \frac{S}{1-\omega} \tag{6}$$

where ω is the crystalline fraction of the said polymer.

PC-SAFT EQUATION OF STATE

The PC-SAFT equation of state for nonassociating molecules is given as an ideal gas contribution (id), a hard-chain contribution (hc), and a perturbation contribution, which accounts for the attractive interactions (disp).

$$Z = Z^{\mathrm{id}} + Z^{\mathrm{hc}} + Z^{\mathrm{disp}} \tag{7}$$

where the compressibility factors, $Z = \mathrm{PV/RT}$ and $Z^{\mathrm{id}} = 1$. The expression of Z^{hc} is identical to the one of Huang and Radosz in the PC-SAFT.[15] The second-order perturbation theory of Barker and Henderson was used to calculate the attractive part of the chain interactions. According to this theory, the Helmholtz free energy is the sum of first- and second-order contribution.

$$\frac{A^{\mathrm{disp}}}{\mathrm{RT}} = \frac{A_1}{\mathrm{RT}} + \frac{A_2}{\mathrm{RT}} \tag{8}$$

where

$$\frac{A_1}{\mathrm{RT}} = -2\pi\rho I_1(\eta,\overline{m})\overline{m^2\ \in\sigma^3} \tag{9}$$

and

$$\frac{A_2}{\mathrm{RT}} = -\pi\rho\overline{m}CI_2(\eta,\overline{m})\overline{m^2\ \in^2\ \sigma^3} \tag{10}$$

with

$$\overline{m} = \text{average segment number of the mixture} = \sum_{i=1}^{\mathrm{nc}} x_i m_i \tag{11}$$

$$\overline{m^2\ \in\sigma^3} = \sum_i\sum_j x_i x_j m_i m_j \left(\frac{\in_{ij}}{kT}\right)\sigma_{ij}^3 \tag{12}$$

$$\overline{m^2\ \in^2\ \sigma^3} = \sum_i\sum_j x_i x_j m_i m_j \left(\frac{\in_{ij}}{kT}\right)^2\sigma_{ij}^3 \tag{13}$$

$$C = \left(1 + \overline{m}\frac{8\eta - 2\eta^2}{(1-\eta)^4} + (1-\overline{m})\frac{20\eta - 27\eta^2 + 12\eta^3 - 2\eta^4}{[(1-\eta)(2-\eta)]^2}\right)^{-1} \tag{14}$$

and $I_1(\eta,\overline{m})$ and $I_2(\eta,\overline{m})$ is a function of $\overline{m}$ and the mixture packing fraction, η, that were reported by Gross and Sadowski.[15] The parameters for a pair of unlike segments are obtained by using conventional Lorentz–Berthelot combining rules.

$$\sigma_{ij} = \frac{1}{2}(\sigma_i + \sigma_j) \tag{15}$$

$$\in_{ij} = \sqrt{\in_i \in_j}\,(1 - \mathrm{Kij}) \tag{16}$$

DOI: 10.1002/apj

The Kij, a binary interaction parameter between components i and j, is introduced to correct the segment–segment interactions of unlike chains. The Z^{hc} is a function of two parameters, the segment number, m_i, and the segment diameter, σ_i and Z^{disp} depend on three parameters, m_i, σ_i, and the segment energy parameter, $\in_i$. Therefore, the PC-SAFT uses three pure-component parameters for each nonassociating molecule. The pure-component parameters of the PC-SAFT equation of state have been taken from the literatures as listed in Table 1.

RESULTS AND DISCUSSION

Effect of molecular weight of polyethylene on solubility

Kobyakov *et al*.[44] studied the solubility of ethylene in two different grades of low density polyethylene (LDPE) with number average molecular weights of 3.65 and 4.95 kg/mol, respectively, under otherwise identical experimental conditions as shown in Fig. 1(a). From the figure, it is clearly observed that the molecular weight of polyethylene has very little effect on the solubility of ethylene at low operating pressures of up to about 100 bars. However, at a pressure higher than 100 bars, the solubility was found to decrease with increasing molecular weight of polyethylene at a fixed temperature. The observed effects of molecular weight of polyethylene on solubility are due to an increase in the incompatibility between the gas and the polymer as the difference in size becomes larger. When the chain length is large enough, the solubility of the gas is expected to be unaffected by the molecular weight

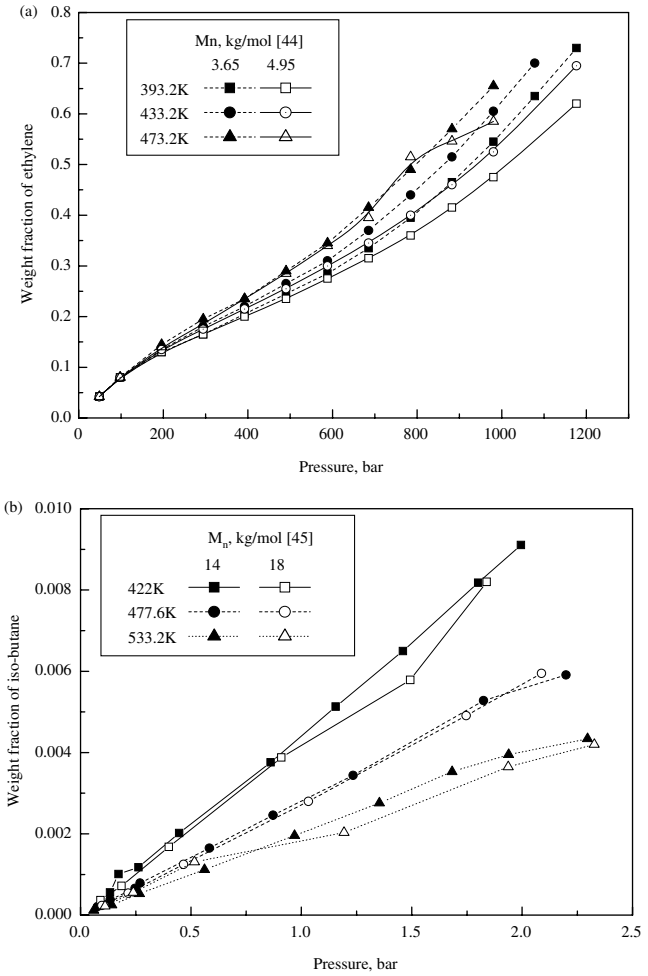

Figure 1. Effect of molecular weight on solubility. (a) Solubility of ethylene in molten LDPE, (b) solubility of iso-butane in molten LDPE.

Table 1. Pure-component parameters of the PC-SAFT equation.

	M, g/mol	m, [−]	σ, [°A]	ε/k, [K]	References
Methane	16.043	1.0000	3.7039	150.03	[15]
Nitrogen	28.01	1.2053	3.3130	90.96	[15]
Carbon dioxide	44.01	2.0729	2.7852	169.21	[15]
Ethylene	28.05	1.5930	3.4450	176.47	[15]
Butane	58.123	2.3316	3.7086	222.88	[15]
Isobutane	58.123	2.2616	3.7574	216.53	[15]
1-Butene	56.107	2.2864	3.6431	222.00	[15]
Propane	44.096	2.0020	3.6184	208.11	[15]
Pentane	72.146	2.6896	3.7729	231.20	[15]
1-Pentene	70.134	2.6006	3.7399	231.99	[15]
Hexane	86.177	3.0576	3.7983	236.77	[15]
1-Hexene	84.616	2.9853	3.7753	236.81	[15]
Heptane	100.203	3.4831	3.8049	238.40	[15]
Cyclopentane	70.13	2.3655	3.7114	265.83	[15]
Polymers		m/M, mol/g	σ, [°A]	ε/k, [K]	
Polyethylene (HDPE)	–	0.0263	4.0217	252.0	[19]
Polyethylene (LDPE)	–	0.0263	4.0217	249.5	[19]

DOI: 10.1002/apj

of the polymer as the gas molecules interact with the polymer at the level of the polymer segments only when they absorb in the liquid phase. Therefore, the absorption isotherms tend to a limiting isotherm as long as the molecular weight of polyethylene is greater than a critical value.

The above statement can be further justified using the solubility data of iso-butane in two different molecular weights of polyethylene, 14 and 18 kg/mol, as shown in Fig. 1(b).[45] As observed from the figure, the effect of molecular weight on solubility is negligible. It is generally accepted that the effect of molecular weight on solubility can be neglected for the molecular weight of the polymers greater than about 5 kg/mol.[32,46] The molecular weight of the polymer was not presented in many of the solubility studies reported in the open literatures (Tables 2 and 3). Therefore, for modeling of the solubility, a reasonable value of molecular weight of polymer greater than 5 kg/mol was assumed when the molecular weight of polyethylene was not reported.

Solubility of ethylene in polyethylene

Cheng and Bonner[47] measured the solubility of ethylene in molten LDPE in the pressure range of up to 70 bars as shown in Fig. 2(a). It is clearly observed from the figure that the solubility of ethylene in molten LDPE decreases with increase in temperature. This is because of the fact that the ethylene becomes more volatile with increasing temperature. In other words, the ethylene–ethylene force of attraction decreases with increase in temperature. However, the high pressure solubility study of ethylene in LDPE shows that the

Table 2. Correlation of Kij with temperature for various gases in polyethylene.

System	T Range	Maximum P	Properties of PE	Kij	ARD	References
Ethylene–LDPE	399.2–428.2	70	$M_n = 31.7$, $M_w = 248.7$, $\rho = 0.9188$	Kij = $-0.175 + 5.5 \times 10^{-04}T$; $R^2 = 0.99$	12.1	[47]
	300–360	35	$M_n = 22$, $M_w = 104$, $\rho = 0.923$, $\omega = 50.4\%$	Kij = $0.166–3.73 \times 10^{-04}T$; $R^2 = 0.94$	1.8	[3]
Ethylene–HDPE	403–495	260	$M_n = 2.2$, $M_w = 2.4$	Kij = $0.0188 + 2.60 \times 10^{-05}T$; $R^2 = 0.98$	3.2	[48]
	300–360	35	$M_n = 11.5$, $M_w = 110.5$, $\rho = 0.954$, $C = 70.2\%$	Kij = $-0.074 + 4.19 \times 10^{-04}T$; $R^2 = 0.79$	5.9	[3]
CO_2–LDPE	423–473	150	$M_n = 15.2$, PI = 6.94, $\rho = 0.919$, $T_m = 375.5$	Kij = $0.0941 + 2.20 \times 10^{-04}T$; $R^2 = 0.99$	1.55	[49]
CO_2–HDPE	433.2–473.3	69–182	$M_n = 8.2$, PI = 13.6, $T_m = 402$	Kij = $-0.1485 + 7.25 \times 10^{-04}T$; $R^2 = 0.99$	2.75	[50]
	298.2–323.2	45	$\rho = 0.954$	Kij = $0.035 + 4.79 \times 10^{-04}T$; $R^2 = 0.99$	1.6	[5]
N_2–LDPE	398.8–499.1	700	$\rho = 0.9209$, $\omega = 52.1\%$	Kij = $-0.085 + 7.26 \times 10^{-04}T$; $R^2 = 0.90$	3.25	[51,52]
N_2–HDPE	433.2–473.3	25–150	$M_n = 8.2$, PI = 13.6, $T_m = 402$	Kij = $0.031 + 4.25 \times 10^{-4}T$; $R^2 = 0.99$	4.5	[50]
CH_4–LDPE	398.4–500.6	60–670	$\rho = 0.9209$, $\omega = 52.1\%$	Kij = $-0.065 + 4.17 \times 10^{-04}T$; $R^2 = 0.99$	11.99	[51]
CH_4–HDPE	298.2–323.2	50–160	$\rho = 0.954$	Kij = $-0.58 + 2.08 \times 10^{-03}T$; $R^2 = 1.0$	4.04	[5]

T, temperature, K; P, pressure, bar; M_n, number average molecular weight, kg/mol; M_w, weight average molecular weight, kg/mol; ρ, density, g/cm^3; ω, crystallinity; PI, polydispersivity index, M_w/M_n; T_m, melting point, K; ARD, Average realtive deviation, % = $\frac{1}{N}\sum_{i=1}^{N}$ ABS(Expt.)$_i$ − $(Model)_i$/(Expt.)$_i$.

DOI: 10.1002/apj

Table 3. Correlation of Kij with temperature for various C_3 to C_7 hydrocarbons in polyethylene.

	T Range	Maximum P	Properties of PE	Kij	ARD	References
n-Propane-HDPE	422–533.2	2	$M_n = 14$, $M_w = 94$, $\rho = 0.951$	Kij = $8.43 \times 10^{-02} - 1.37 \times 10^{-04}T$; $R^2 = 0.84$	3.2	[45]
n-Butane-LDPE	383–473	35	$T_m = 382.7$, MFR = 2.3 g/10 min	Kij = $6.68 \times 10^{-03} + 1.07 \times 10^{-05}T$; $R^2 = 0.63$	1.14	[1]
Iso-butane-LDPE	383–473	30	$T_m = 382.7$, MFR = 2.3	Kij = $-2.059 \times 10^{-04} + 2.83 \times 10^{-05}T$; $R^2 = 0.55$	0.91	[1]
1-Butene-LDPE	493	75	$M_n = 1.94$, $M_w = 5.37$, $\rho = 0.9238$	–	3.93	[53]
n-Butane-LDPE	258–313	0.9	$M_n = 24.9$, PI = 3, $\rho = 0.9157$, $\omega = 43\%$	Kij = $-0.316 + 2.5 \times 10^{-03}T - 4.4 \times 10^{-06}T^2$; $R^2 = 0.71$	6.12	[54]
1-Butene-LDPE	303–361	12	$M_n = 22$, $M_w = 104$, $\rho = 0.923$, $\omega = 50.4\%$	Kij = $0.18 - 4.67 \times 10^{-04}T$; $R^2 = 0.93$	4.7	[3]
1-Butene-HDPE	303–361	12	$M_n = 11.5$, $M_w = 110.5$, $\rho = 0.954$, $\omega = 70.2\%$	Kij = $0.097–1.593 \times 10^{-04}T$; $R^2 = 0.92$	7.98	[3]
n-Pentane-LDPE	263–308	0.6	$M_n = 24.9$, PI = 3, $\rho = 0.9157$, $\omega = 43\%$	Kij = $-0.66 + 4.95 \times 10^{-03}T - 8.9 \times 10^{-06}T^2$; $R^2 = 0.88$	9.40	[54]
n-Pentane-LDPE	423–474	30	$M_n = 7.6$, $\rho = 0.919$, PI = 6.91	–	3.76	[55]
1-Pentene-LDPE	423–474	32	$M_n = 7.6$, $\rho = 0.919$, PI = 6.91	–	3.35	[55]
n-Hexane-LDPE	273–313	0.2	$M_n = 24.9$, PI = 3, $\rho = 0.9157$, $\omega = 43\%$	Kij = $-0.24 + 1.94 \times 10^{-03}T - 3.44 \times 10^{-6}T^2$; $R^2 = 0.89$	14.0	[54]
1-Hexene-LDPE	342–361	2	$M_n = 22$, $M_w = 104$, $\rho = 0.923$, $\omega = 50.4\%$	–	13.95%	[3]
1-Hexene-HDPE	342–361	2	$M_n = 11.5$, $M_w = 110.5$, $\rho = 0.954$, $\omega = 70.2\%$	–	6.45	[3]
n-Heptane-LDPE	288–318	0.04	$M_n = 24.9$, PI = 3, $\rho = 0.9157$, $\omega = 43\%$	Kij = $-0.24 + 194 \times 10^{-03}T - 3.44 \times 10^{-6}T^2$; $R^2 = 0.89$	14.0	[54]
Cyclopentane-LDPE	425–474	23	$M_n = 76$, MI = 65, $\rho = 0.919$	–	1.67	[55]

MFR, melt flow rate (g/10 min); MI, melt index. All other abbreviations are same as in Table 2.

solubility increases with increase in temperature above a certain pressure as shown in Fig. 2(b).[44] Bocdanovic *et al*.[56] also reported the similar inversion trends of solubility of ethylene in polyethylene. It may be further observed from the figures that the nature of the absorption isotherm becomes concave upward above inversion pressure although it is almost linear at pressures below the inversion pressure. The possible explanation for these observations may be ethylene–ethylene interaction is attractive in nature and comparable to the ethylene–polyethylene interaction force below the inversion pressure and hence the amount of absorption increases linearly with pressure following the Henry's law.[32] However, as the pressure increases above the inversion pressure, ethylene–ethylene attractive force becomes significant and more favorable than the ethylene–polyethylene interaction force. As a consequence, ethylene molecules present in liquid phase attract more ethylene molecules into it and the solubility increases progressively resulting in the concave upward nature of the absorption isotherm. The ethylene–ethylene attractive force relative to ethylene–polyethylene possibly decreases with temperature above the inversion

DOI: 10.1002/apj

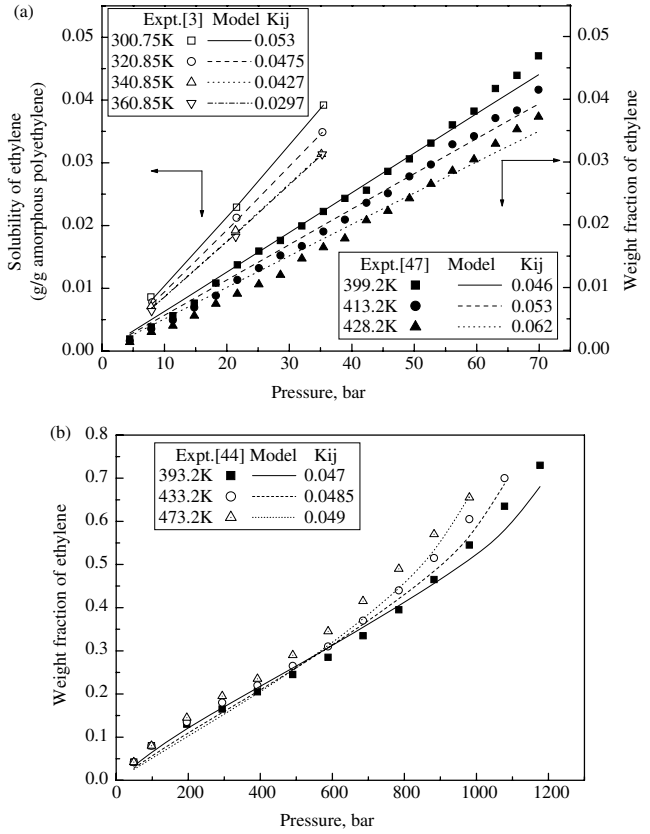

Figure 2. Solubility of ethylene in LDPE.

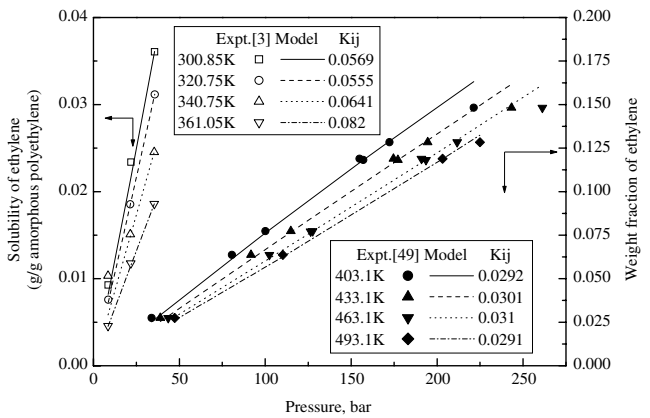

Figure 3. Solubility of ethylene in HDPE.

pressure, resulting in an increase in the absorption of ethylene into polyethylene at higher temperature.[32]

Rousseaux *et al*.[48] studied the solubility of ethylene in molten high density polyethylene (HDPE), as shown in Fig. 3. The solubility of ethylene in molten HDPE, however, decreases with increase in temperature as one can observe from the figure. The study of solubility of ethylene in semicrystalline polyethylene below the crystalline melting temperature is limited in literatures. Moore and Wanke[3] studied the solubility of ethylene in semicrystalline LDPE and HDPE up to 35 bar pressure in the temperature range of 300–360 K. In case of semicrystalline polyethylene, the solubility of ethylene decreases with increase in temperature for both LDPE and HDPE and the absorption isotherm is linear as shown in Figs 2(a) and 3, respectively.

The binary interaction parameter, Kij, of PC-SAFT at different temperatures has been estimated by regression of the PC-SAFT model using the available experimental solubility isotherm for ethylene in both molten and semicrystalline LDPE and HDPE (Figs. 2 and 3). The objective function, E, minimized is given below by Eqn 17.

$$E = \sum_{i=1}^{n} \left[S_i^{\text{expt}} - S_i^{\text{cal}} \right]^2 \tag{17}$$

where S is the equilibrium weight fraction of ethylene in polyethylene. The solubility calculated based on the developed model using the estimated values of Kij was compared with the experimental data (Figs. 2 and 3). The developed model based on PC-SAFT correlates the experimental data with only a minor adjustment of Kij. Furthermore, a suitable correlation of Kij with temperature was developed as shown in Table 2.

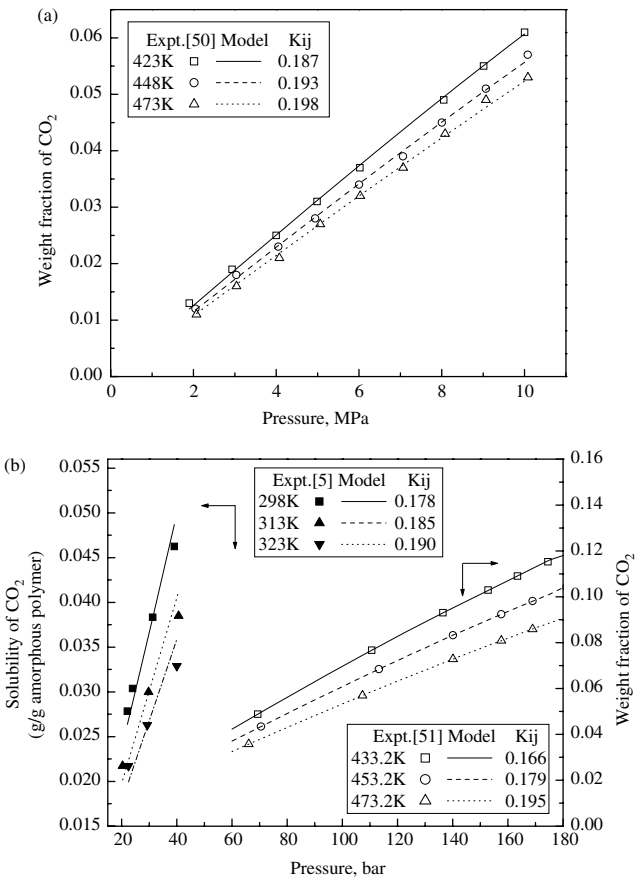

Figure 4. Solubility of CO_2 in polyethylene. (a) LDPE, (b) HDPE.

DOI: 10.1002/apj

Solubility of CO_2 in polyethylene

Areerat *et al*. and Sato *et al*.[49,50] measured the solubility of CO_2 in molten LDPE and HDPE, respectively (Fig. 4). Solms *et al*.[5] presented the solubility of CO_2 in semicrystalline HDPE per unit mass of total polymer. As absorption of gases is limited to only the amorphous region of the semicrystalline polymer, the crystalline fraction (ω) of the HDPE was calculated using the reported density of polyethylene of 0.954 g/cm^3 (Table 2) based on following relation.[32]

$$\omega = \left(\frac{\rho_{pol} - \rho_{am}}{\rho_{crys} - \rho_{am}}\right)\left(\frac{\rho_{crys}}{\rho_{pol}}\right) \quad (18)$$

where ρ_{pol}, ρ_{am}, and ρ_{crys} represent densities of the polymer sample, fully amorphous, and completely crystalline polymer measured at 298 K, respectively. For polyethylene, the values of ρ_{am} and ρ_{crys} are 0.862 g/cm^3 and 1.005 g/cm^3, respectively.[32] Using the calculated value of ω (= 0.677), the experimental absorption data were normalized per unit mass of amorphous polymer and Kij were then estimated at different temperatures by regression of the PC-SAFT model using these normalized data. The estimated values of Kij were found to be very close to that of molten HDPE as shown in Fig. 4.

The absorption of CO_2 was found to be linearly increasing with pressure for both molten LDPE and HDPE and semicrystalline HDPE under the experimental conditions studied, as observed from the figures. The solubility of CO_2 was found to decrease with increase in temperature. The comparison of experimental data with that of model-based prediction using optimized Kij shows a reasonably good correlation (Fig. 4). The developed correlations of Kij with temperature for both molten and semicrystalline LDPE and HDPE are shown in Table 2.

Solubility of nitrogen in polyethylene

Lundberg *et al*. and Cheng[51,52] studied the solubility of nitrogen in molten LDPE. Sato *et al*.[50] also reported the solubility of nitrogen gas in molten HDPE. However, the solubility of nitrogen in semicrystalline polyethylene has not been reported so far in open literature. The comparison of the correlated results based on the developed model using estimated Kij at different temperatures with that of experimental results are shown in Fig. 5. It is interesting to note that the solubility of nitrogen increases with increase in temperature for both LDPE and HDPE. Moreover, it may be observed from the figure that the nature of absorption isotherm is convex downward.

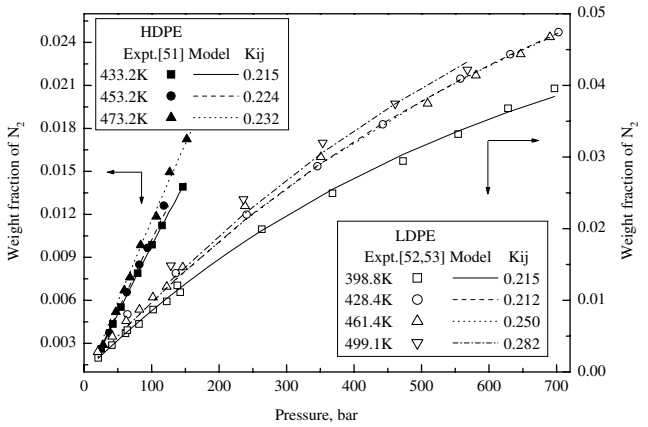

Figure 5. Solubility of nitrogen in polyethylene.

The nitrogen–nitrogen interaction is known to be repulsive in nature. However, the presence of nitrogen in the liquid phase results in a repulsive force for further absorption of nitrogen leading to a convex downward nature of solubility isotherm. Moreover, the nitrogen–nitrogen repulsive force decreases with increase in temperature, which results in increased absorption of nitrogen at higher temperatures.[32] Furthermore, a suitable correlation of Kij with temperature was developed as shown in Table 2 and the developed model based on PC-SAFT equation of state correlates the experimental results very well.

Solubility of methane in polyethylene

The solubility of CH_4 was reported only in molten LDPE[51] and semicrystalline HDPE[5] as shown in Fig. 6. The experimental absorption data for semicrystalline HDPE has also been normalized per unit mass of amorphous polymer similar to that of CO_2–HDPE system using Eqn 18. The solubility of CH_4 in molten LDPE was found to increase with increase in temperature; the opposite trend was reported for semicrystalline HDPE. However, the convex downward nature of the absorption isotherm was observed in both cases, similar to that of the N_2-polyethylene system. Comparison of experimental data and model-based correlation based on optimized values of Kij at different temperatures is shown in Fig. 6 and corresponding correlations of Kij with temperatures are shown in Table 2.

Solubility of C_3 to C_7 hydrocarbons in polyethylene

The developed model based on the PC-SAFT equation of state was tested using the available experimental data

DOI: 10.1002/apj

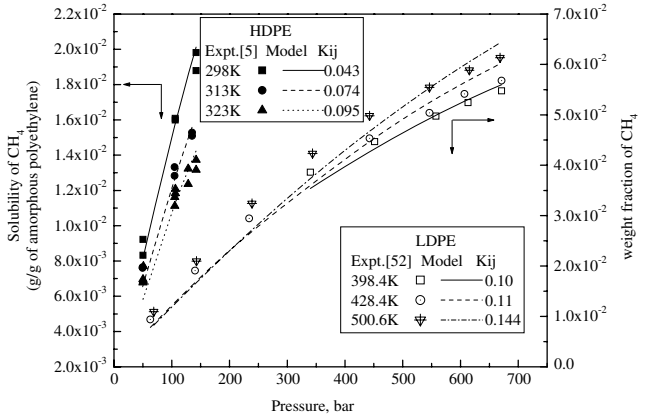

Figure 6. Solubility of methane in polyethylene.

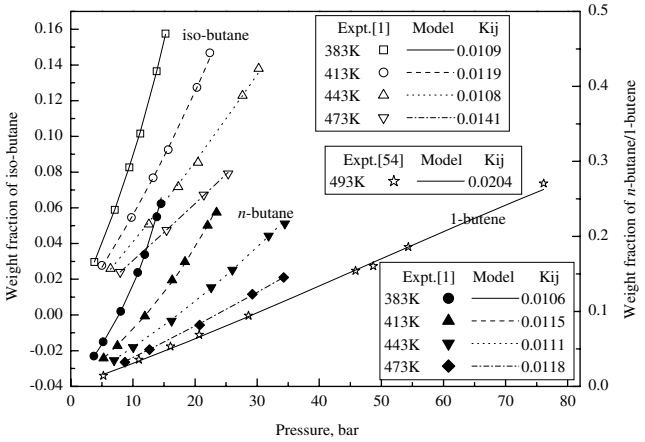

Figure 7. Solubility of *n*-butane, iso-butene, and 1-butene in molten LDPE.

in literatures for C_3 to C_7 hydrocarbons in polyethylene as shown in Figs 7–13. Meyer and Blanks[45] studied the solubility of *n*-propane in molten HDPE as shown in Fig. 10. Wang *et al*.[1] reported the solubility of *n*-butane and iso-butane in molten LDPE as shown in Fig. 7. Wohlfarth *et al*.[53] studied the solubility of 1-butene in molten LDPE at single temperature, 493 K, as shown in Fig. 7. Castro *et al*.[54] studied the solubility of *n*-butane in semicrystalline LDPE for a wide range of temperatures as shown in Fig. 8. Fig. 9 shows the solubility results of 1-butene in two different types of semicrystalline polyethylene, LDPE and HDPE.[3] Surana *et al*.[55] studied the solubility of *n*-pentane and 1-penetene in molten LDPE as shown in Fig. 11. Castro *et al*.[54] studied the solubility of *n*-pentane in semicrystalline LDPE as shown in Fig. 10. Castro *et al*.[54] studied the solubility of *n*-hexane in semicrystalline LDPE as shown in Fig. 12. The solubility of 1-hexene in semicrystalline LDPE and HDPE was reported by Moore and Wanke,[3] as shown in the same figure. Castro *et al*.[54] reported the solubility of *n*-heptane in semicrystalline LDPE as shown in Fig. 13. As observed from the Figs 7–13, the solubility of C_3 to C_7 hydrocarbons was found to decrease with increasing temperature for both molten and semicrystalline polyethylene. This is because of the fact that the condensability decreases with increasing temperature.

The nature of solubility isotherms for *n*-propane is almost linear with pressure as observed from Fig. 10. However, the nature of the solubility isotherm in all other cases was found to be concave upward as observed from the figures. From these observations, it may be concluded that the interaction force among C_4 to C_7 hydrocarbon molecules is more favorable than hydrocarbon–polyethylene interaction. As C_4 to C_7 hydrocarbon absorb into polyethylene, it attracts more hydrocarbon because of the strong force of attraction that results in the concave nature of solubility isotherm.[32]

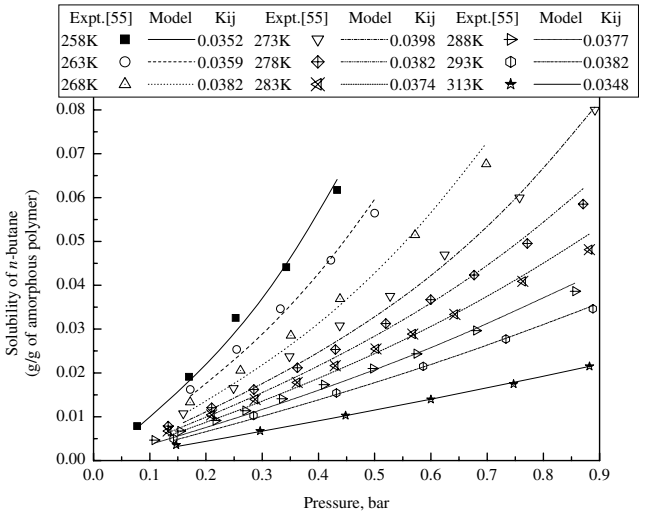

Figure 8. Solubility of *n*-butane in semicrystalline LDPE.

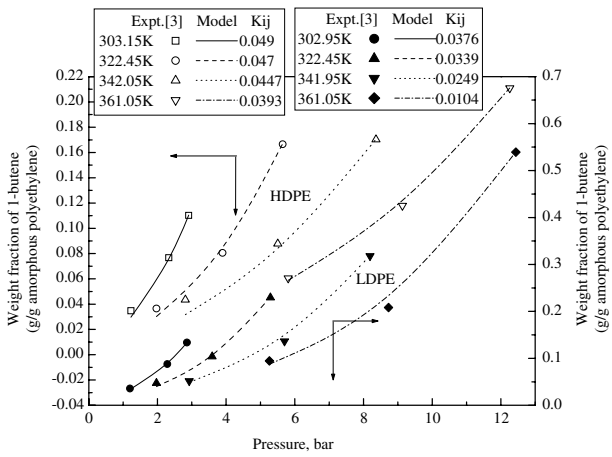

Figure 9. Solubility of 1-butene in semicrystalline LDPE and HDPE.

DOI: 10.1002/apj

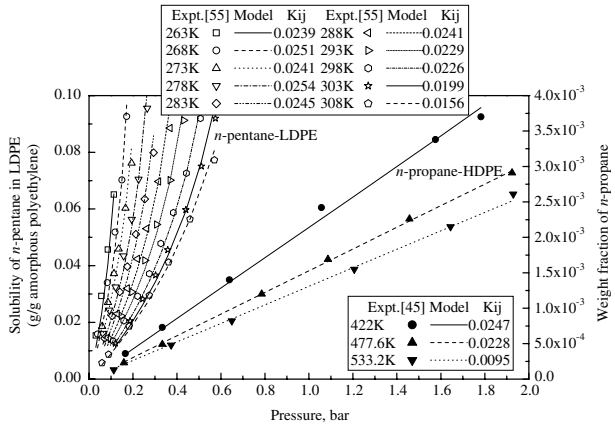

Figure 10. Solubility of *n*-propane in molten HDPE and *n*-pentane in semicrystalline LDPE.

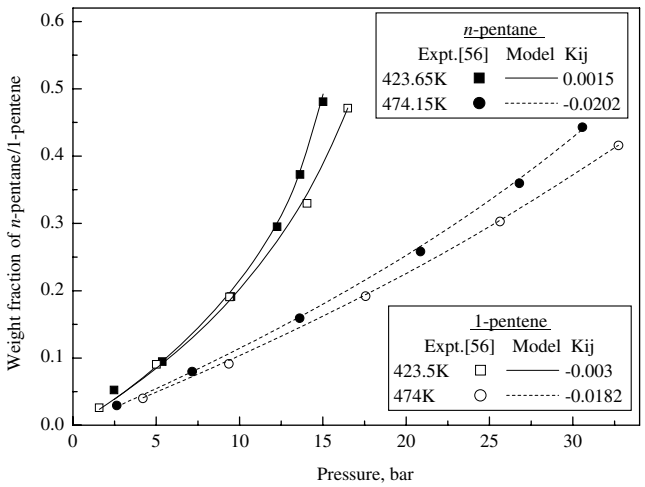

Figure 11. Solubility of *n*-pentane and 1-penetene in molten LDPE.

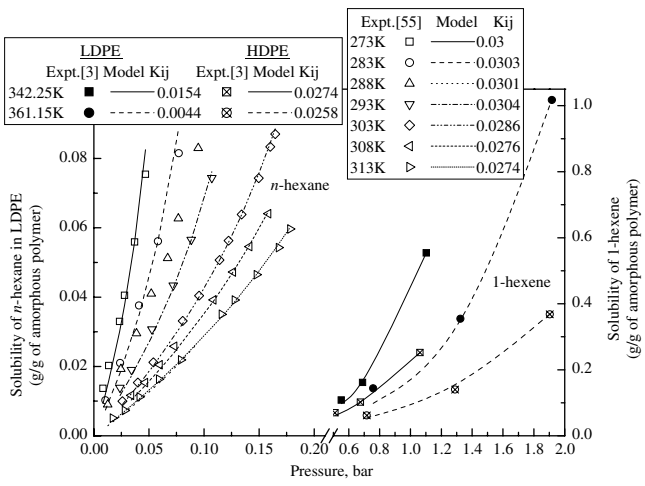

Figure 12. Solubility of *n*-hexane in semicrystalline LDPE and 1-hexene in semicrystalline LDPE and HDPE.

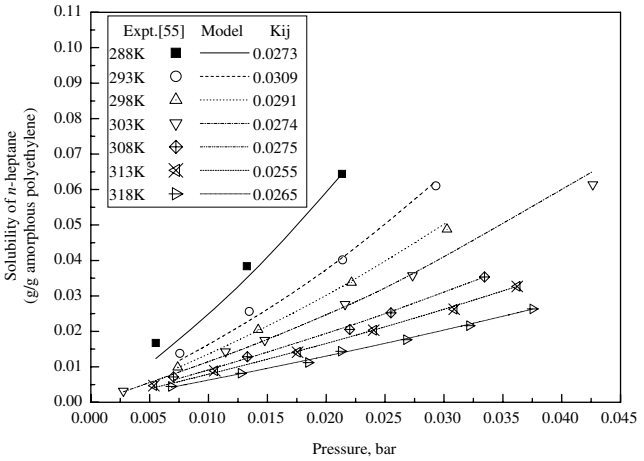

Figure 13. Solubility of *n*-heptane in semicrystalline LDPE.

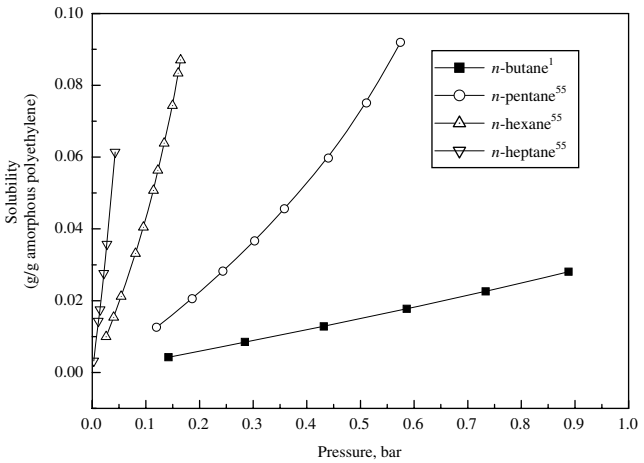

Figure 14. Comparison of solubility of hydrocarbons in semicrystalline LDPE at 303 K.

The experimental solubility of linear hydrocarbons in semicrystalline LDPE was compared at the same temperature, 303 K, as shown in Fig. 14. It is clearly observed from the figure that solubility increases with increasing molecular weight of hydrocarbons. This may be due to the fact that the condensability increases with the increase in molecular weight of hydrocarbons. The solubility of *n*-butane is greater than iso-butane in molten LDPE at the same temperature as observed from Fig. 7. Moreover, the solubility of *n*-pentane is higher than 1-pentene in molten LDPE as observed from Fig. 11. The solubility of 1-butene was found to be more in semicrystalline LDPE compared with that in HDPE as shown in Fig. 9. The solubility of 1-hexene in semicrystalline LDPE was found to be higher than that in HDPE as observed from the Fig. 12. This information is quite useful for consideration of gases for practical foaming processes.

Using the available experimental solubility data in literatures, the binary interaction parameters (Kij) of

DOI: 10.1002/apj

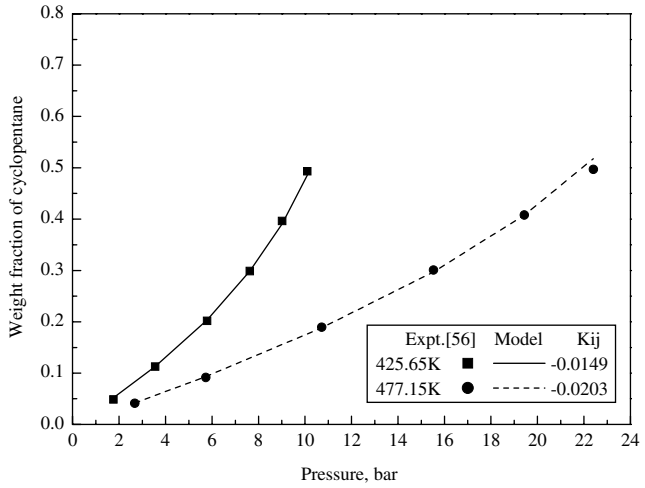

Figure 15. Solubility of cyclopentane in molten LDPE.

the PC-SAFT equation of state for different hydrocarbon–polyethylene systems were estimated at different temperatures as shown in the figure captions of the respective figures. Using the estimated Kij values, the solubility of hydrocarbons was calculated at different temperatures and compared to that of experimental solubility data as shown in Figs 7–13. The developed model based on PC-SAFT correlates the experimental data reasonably well, as observed from the figures. Finally, a suitable correlation of Kij with temperature was developed for different hydrocarbon–polyethylene systems as shown in Table 3.

Solubility of cyclopentane

The experimental solubility of cyclopentane in molten LDPE and comparison with that of model is presented in Fig. 15.[55] The solubility was found to decrease with increasing temperature and the nature of the solubility isotherm is concave upward as observed in the case of hydrocarbons. A similar explanation may be used to explain the nature of the isotherm.

CONCLUSIONS

The solubility of various gases such as ethylene, carbon dioxide, nitrogen, and methane and hydrocarbons of up to chain length of seven in polyethylene below and above the melting point was suitably correlated using a thermodynamic model based on the PC-SAFT equation of state. The optimum values of adjustable solvents–solute binary interaction parameters (Kij) of PC-SAFT at different temperatures have been estimated using the available solubility data for various gases and hydrocarbons and a suitable correlation of Kij with temperature was then developed. The calculated solubility results using the estimated Kij were then compared to experimental data and a reasonably good correlation was observed in all systems. The review of available solubility data for various gases and hydrocarbons in polyethylene revealed the following trends.

- The solubility was found to increase with increasing temperature for N_2-polyethylene (molten), CH_4–LDPE (molten), and ethylene–LDPE (molten) system above the inversion pressure.
- The convex downward nature of the solubility isotherm was observed for N_2-polyethylene (molten) and CH_4–LDPE systems. The convex upward nature of the solubility isotherm was observed for all C_3 to C_7 hydrocarbon polyethylene systems except for *n*-propane.
- The solubility was found to increase with the molecular weight of hydrocarbons. The solubility of gases was found to be higher in LDPE compared with that in HDPE. Unsaturated hydrocarbons show higher solubility compared with saturated hydrocarbons.

NOMENCLATURE

Abbreviations

A	Helmholtz free energy
f	Fugacity coefficient
Kij	Binary interaction parameter of PC-SAFT
T	Temperature
T_m	Melting point
M	Molecular weight
m	Number of segments
M_n	Number average molecular weight
M_w	Weight average molecular weight
MI	Melt index
MFR	Melt flow rate
$\overline{m}$	Average segment number of the mixture
PI	Polydispersivity index
P	Pressure
S	Solubility per unit mass of polymer
w	Solubility in weight fraction
x	Mole fraction in liquid phase
y	Mole fraction in vapor phase
Z	Compressibility factors

Greek letters

ϕ	Fugacity coefficient
ω	Crystallinity
ρ	Density
ε/k	Interaction energy
σ	Segment diameter
η	Mixture packing fraction

DOI: 10.1002/apj

Superscripts

disp	Perturbation contribution
G	Gas phase
hc	Hard-chain contribution
id	Ideal gas contribution
L	Liquid phase

Subscripts

am	Amorphous
cal	Calculated
crys	Crystalline
expt	Experimental
i	Component
pol	Polymer

REFERENCES

[1] M. Wang, Y. Sato, T. Iketani, S. Takishima, H. Masuoka, T. Watanabe, Y. Fukasaw. *Fluid Phase Equilib.,* **2005;** *232*, 1–8.
[2] Y. Sato, A. Tsuboi, A. Sorakubo, S. Takishima, H. Masuoka, T. Ishikawa. *Fluid Phase Equilib.,* **2000;** *17*, 49–67.
[3] S.J. Moore, S.E. Wanke. *Chem. Eng. Sci.,* **2001;** *56*, 4121–4129.
[4] R.W. Baker. *Membrane Technology and Applications*, John Wiley & Sons Ltd.: England, **2004**.
[5] N. von Solms, J.K. Nielsen, O. Hassager, A. Rubin, A.Y. Dandekar, S.I. Andersen, E.H. Stenby. *J. Appl. Polym. Sci.,* **2004;** *91*, 1476–1488.
[6] P.J. Flory. *J. Chem. Phys.,* **1942;** *10*, 51–61.
[7] I.C. Sanchez, R.H. Lacombe. *J. Phys. Chem.,* **1976;** *80*, 2352–2362.
[8] I. Nagya, T.D. Loos, R. Krenz, R. Heidemann. *J. Supercrit. Fluids,* **2006;** *37*, 115–124.
[9] W.G. Chapman, K.E. Gubbins, G. Jackson, M. Radosz. *Ind. Eng. Chem. Res.,* **1990;** *29*, 1709–1721.
[10] A. Galindo, P.J. Whitehead, G. Jackson. *J. Phys. Chem.,* **1996;** *100*, 6781–6792.
[11] A. Galindo, P.J. Whitehead, G. Jackson, A.B. Burgess. *J. Phys. Chem. B,* **1997;** *101*, 2082–2091.
[12] Y.H. Fu, S.I. Sandler. *Ind. Eng. Chem. Res.,* **1995;** *34*, 1897–1909.
[13] T. Kraska, K.E. Gubbins. *Ind. Eng. Chem. Res.,* **1996;** *35*, 4727–4737.
[14] T. Kraska, K.E. Gubbins. *Ind. Eng. Chem. Res.,* **1996;** *35*, 4738–4746.
[15] J. Gross, G. Sadowski. *Ind. Eng. Chem. Res.,* **2001;** *40*, 1244–1260.
[16] A. Gil-Villegas, A. Galindo, P.J. Whitehead, S.J. Mills, G. Jackson, A.N. Burgess. *J. Chem. Phys.,* **1997;** *106*, 4168–4186.
[17] N. von Solms, M.L. Michelsen, G.M. Kontogeorgis. *Ind. Eng. Chem. Res.,* **2003;** *42*, 1098–1105.
[18] J. Gross, G. Sadowski. *Ind. Eng. Chem. Res.,* **2002;** *41*, 1084–1093.
[19] F. Tumakaka, J. Gross, G. Sadowski. *Fluid Phase Equilib.,* **2002;** *194–197*, 541–551.
[20] J. Gross, G. Sadowski. *Ind. Eng. Chem. Res.,* **2002;** *41*, 5510–5515.
[21] J. Gross, O. Spuhl, F. Tumakaka, G. Sadowski. *Ind. Eng. Chem. Res.,* **2003;** *42*, 1266–1274.
[22] F. Tumakaka, G. Sadowski. *Fluid Phase Equilib.,* **2004;** *217*, 233–239.
[23] P.K. Jog, W.G. Chapman, S.K. Gupta, R.D. Swindoll. *Ind. Eng. Chem. Res.,* **2002;** *41*, 887–891.
[24] T. Spyriouni, I.G. Economou. *Polymer,* **2005;** *46*, 10772–10781.
[25] N. Pedrosa, L.F. Vega, J.A.P. Coutinho, I.M. Marrucho. *Macromolecules,* **2006;** *39*, 4240–4246.
[26] P.F. Arce, M. Aznar. *J. Supercrit. Fluids,* **2008;** *43*, 408–420.
[27] R. Agarwal, D. Prasad, S. Maity, K. Gayen, S. Ganguly. *J. Chem. Eng. Jpn.,* **2004;** *37*, 1427–1435.
[28] F. Becker, M. Buback, H. Latz, G. Sadowski, F. Tumakaka. *Fluid Phase Equilib.,* **2004;** *215*, 263–282.
[29] F. Tumakaka, G. Sadowski, H. Latz, M. Buback. *J. Supercrit. Fluids,* **2007;** *41*, 461–471.
[30] A.J. Haslam, N. von Solms, C.S. Adjiman, A. Galindo, G. Jackson, P. Paricaud, M.L. Michelsen, G.M. Kontogeorgis. *Fluid Phase Equilib.,* **2006;** *243*, 74–91.
[31] N. von Solms, M.L. Michelsen, G.M. Kontogeorgis. *Ind. Eng. Chem. Res.,* **2005;** *44*, 3330–3335.
[32] P. Paricaud, A. Galindo, G. Jackson. *Ind. Eng. Chem. Res.,* **2004;** *43*, 6871–6889.
[33] D.N. Justo-García, F. García-Sánchez, N.L. Díaz-Ramírez, A. Romero-Martínez. *Fluid Phase Equilib.,* **2008;** *265*, 192–204.
[34] P. Arce, M. Aznar. *J. Supercrit. Fluids,* **2008;** *45*, 134–145.
[35] M.F. Alfradique, M. Castier. *Fluid Phase Equilib.,* **2007;** *257*, 78–101.
[36] S.P. Tan, H. Adidharma, B.F. Towler, M. Radosz. *Ind. Eng. Chem. Res.,* **2006;** *45*, 2116–2122.
[37] D. Fu, X.S. Li, S.M. Yan, T. Liao. *Ind. Eng. Chem. Res.,* **2006;** *45*, 8199–8206.
[38] S. Grob, H. Hasse. *J. Chem. Eng. Data,* **2005;** *50*, 92–101.
[39] S. Grob, H. Hasse. *Ind. Eng. Chem. Res.,* **2006;** *45*, 1869–1874.
[40] S. Aparicio-Martínez, K.R. Hall. *Ind. Eng. Chem. Res.,* **2007;** *46*, 273–284.
[41] S. Beret, S.L. Hager. *J. Appl. Polym. Sci.,* **1979;** *24*, 1787–1796.
[42] R.A. Hutchinson, W.H. Ray. *J. Appl. Polym. Sci.,* **1990;** *41*, 51–81.
[43] W. Yao, X. Hu, Y. Yan. *J. Appl. Polym. Sci.,* **2007;** *103*, 1737–1744.
[44] V.M. Kobyakov, V.B. Kogan, V.S. Zernov. *Zh. Prikl. Khim.,* **1987;** *60*, 81.
[45] J.A. Meyer, R.F. Blanks. *J. Appl. Polym. Sci.,* **1983;** *28*, 725.
[46] C.J. Peng, H.L. Liu, Y. Hu. *Chem. Eng. Sci.,* **2001;** *56*, 6967–6975.
[47] Y.L. Cheng, D.C. Bonner. *J. Polym. Sci.: Polym. Phys. Ed.,* **1977;** *15*, 593–603.
[48] P. Rousseaux, D. Richon, H. Renon. *J. Polym. Sci.: Polym. Chem. Ed.,* **1985;** *23*, 1771–1785.
[49] S. Areerat, Y. Hayata, R. Katsumoto, T. Kegaswaa, H. Engami, M. Ohshima. *J. Appl. Polym. Sci.,* **2002;** *86*, 282–288.
[50] Y. Sato, K. Fujiwara, T. Takikawa, T.S. Sumarno, H. Masuoka. *Fluid Phase Equilib.,* **1999;** *162*, 261–276.
[51] J.L. Lundberg, M.B. Wilk, M.J. Huyett. *J. Polym. Sci.,* **1962;** *57*, 275–299.
[52] Y.L. Cheng. *J. Polym. Sci.: Polym. Phys. Ed.,* **1978;** *16*, 319–333.
[53] C. Wohlfarth, U. Finck, R. Schultz, T. Heuer. *Angew. Makromol. Chem.,* **1992;** *198*, 91.
[54] E.F. Castro, E.E. Gonzo, J.C. Gottifredi. *J. Membr. Sci.,* **1987;** *31*, 235–248.
[55] R.K. Surana, R.P. Danner, A.B. de Haan, N. Beckers. *Fluid Phase Equilib.,* **1997;** *139*, 361–370.
[56] V.Ž. Bocdanovic, A.Ž. Tasiæ, B.D. Djordjevic. *J. Appl. Polym. Sci.,* **1990;** *41*, 3091–3095.

DOI: 10.1002/apj